

molecule with a loosely bound electron was found in the matrix. This can easily be understood from the calculated gas-phase curve for the  $\text{HCl}^-$  ion.

The energy difference between the two minima for  $\text{HCl}^-$  is only 8.3 kcal/mol whereas the energy difference between the minimum energy geometry and the dissociated  $\text{H} + \text{F}^-$  system is 57.4 kcal. Thus when the effect of the dielectric surrounding is included for  $\text{HCl}^-$ , the minimum corresponding to a  $\text{HCl}$  molecule that has bound an electron in a diffuse orbital has been swallowed by the  $\text{H} + \text{Cl}^-$  ion minimum.

#### Comparison with Experimental Results Obtained for $\text{HF}^-$ and $\text{HCl}^-$ in Matrices

In recent work Raynor et al.<sup>9</sup> have studied the  $\text{HF}^-$ ,  $\text{HCl}^-$ ,  $\text{HBr}^-$ , and  $\text{HI}^-$  species in a  $\text{Me}_3\text{NSO}_3$  matrix by ESR measurements. The  $\text{HX}^-$  ( $\text{X} = \text{F}, \text{Cl}, \text{Br}, \text{I}$ ) system is created by doping the  $\text{Me}_3\text{NSO}_3$  matrix with  $\text{Me}_3\text{NHX}$  and irradiating the system with  $\gamma$ -radiation. From their study they conclude that in both cases the electronic structure of the species corresponds to a halide ion and a hydrogen atom. When the halide ion is fluorine, the unpaired electron is completely localized on the hydrogen atom, but when another halide ion is used, there is a small but significant delocalization of the unpaired electron onto the halide. Furthermore, the authors were able to detect a hindered rotation of the hydrogen atom when the halide is  $\text{Cl}$  or  $\text{Br}$ . In order to be able to compare the experimentally observed data with that calculated, one must assume something about the flexibility of the matrix. To get some grip on this problem, it seems fruitful to consider the two limiting possibilities: (i) that the matrix adjusts itself like a liquid around the  $\text{HX}^-$  system or (ii) that the matrix is stiff and that the size of the hole in the matrix is fixed. If the

matrix were soft, the quantum chemical calculations presented here indicates that the  $\text{HF}^-$  ion would be a  $\text{HF}$  molecule that had captured an electron, in contradiction with experiment. It would further be difficult to rationalize the hindered rotation observed for  $\text{HCl}^-$  or  $\text{HBr}^-$ . If we, however, make the opposite assumption that the size of cavity is more or less fixed and given by the volume of the  $\text{SO}_3$  molecule in the matrix, then theory and experiments agree well. It seems reasonable to assume that the volume of a  $\text{SO}_3$  group can be regarded as a sphere with a radius of 3.8 Å. Under these conditions the  $\text{HCl}^-$  or  $\text{HF}^-$  ion prefers an electronic structure corresponding to a  $\text{H}$  atom and a  $\text{X}^-$  ion, whereas an  $\text{HX}$  molecule would have needed a cavity with a radius of  $\sim 7$  Å. Furthermore, the cavity is large enough to allow for the electron clouds of the hydrogen atom and the  $\text{F}^-$  ion not to overlap significantly. A small overlap will, however, be present for the  $\text{HCl}^-$  system. It is further easy to imagine that there is ample space for the  $\text{H}$  atom to move around when a  $\text{F}^-$  ion is present, but when  $\text{Cl}^-$  or  $\text{Br}^-$  is in the cavity, then this motion is hindered as is experimentally observed, and when  $\text{I}^-$  is used this motion is quenched.

Thus we may conclude that if the size of the cavity is kept almost constant, there is good agreement between experimentally observed data on the  $\text{HX}^-$  systems in  $\text{Me}_3\text{NSO}_3$  matrices and quantum chemical dielectric medium calculations.

A model that is as crude as the one used in this work obviously cannot give an exact answer to questions concerning the electronic structure of molecules in condensed phases, but it can certainly be of good help in the interpretation of experimental data and indicate possibilities and trends.

**Registry No.**  $\text{HF}$ , 7664-39-3;  $\text{HF}^-$ , 37249-79-9;  $\text{HCl}$ , 7647-01-0;  $\text{HCl}^-$ , 63099-75-2.

## Broad-Band Ultrasonic Absorption Spectroscopy of an Isobutyric Acid/Water Mixture of Critical Composition

U. Kaatz\* and U. Schreiber

*Drittes Physikalisches Institut, Universität Göttingen, Bürgerstrasse 42-44, D-3400 Göttingen, West Germany*  
(Received: September 9, 1988)

Between 0.2 and 400 MHz the dependence upon frequency of the ultrasonic absorption coefficient has been measured for (a) an isobutyric acid/water mixture of critical composition as a function of temperature, (b) a dilute aqueous solution of isobutyric acid at 25 °C, and (c) the pure acid at the same temperature. The excess absorption spectra for the dilute solution and for the pure carboxylic acid show Debye-type relaxation behavior. The relaxation times are 3.3 and 24 ns, respectively. The excess absorption spectrum for the mixture of critical composition is uncommonly broad. It can be described by a superposition of two relaxation spectral functions, one with a Cole-Cole relaxation time distribution, the other one with a discrete relaxation time. Attempts failed to apply theoretically predicted expressions which consider the contributions from local fluctuations in concentration near the critical point. The parameters of the low-frequency relaxation term distinctly depend on the temperature. The high-frequency Debye process is assumed to be due to dimerization of the acid.

### Introduction

There is a current wide interest toward the thermodynamic and transport properties of fluids near a critical point. This interest was additionally stimulated in 1981 by a theoretical work of Procaccia and Gitterman<sup>1</sup> who asserted that the rates of chemical reactions might show characteristic anomalies when the system approaches its critical point ("critical slowing down"). Two years later, Dunker et al.<sup>2</sup> studied the ultrasonic absorption of the reactive binary liquid isobutyric acid/water near the consolute

critical point. They analyzed their data assuming the total absorption per wavelength,  $\alpha\lambda$ , to be representable by a sum

$$\alpha\lambda = (\alpha\lambda)^{\text{cl}} + (\alpha\lambda)^{\text{cf}} + \sum_{n=1}^N (\alpha\lambda)_n^{\text{ch}} \quad (1)$$

Herein,  $(\alpha\lambda)^{\text{cl}}$  denotes the so-called classical contribution as due to thermal conductivity and internal viscous friction,  $(\alpha\lambda)^{\text{cf}}$  is the part resulting from concentration fluctuations, and terms  $(\alpha\lambda)_n^{\text{ch}}$ ,  $n = 1, \dots, N$ , reflect the chemical reactions that are taking place in the solution. Due to the limited range of frequencies of measurement (9–45 MHz) Dunker et al. used one  $(\alpha\lambda)^{\text{ch}}$  term only ( $N = 1$  in eq 1). They found indications to assume this part of the absorption per wavelength to reflect chemical slowing.

(1) Procaccia, I.; Gitterman, M. *Phys. Rev. Lett.* **1981**, *46*, 1163.

(2) Dunker, H.; Woermann, D.; Bhattacharjee, J. K. *Ber. Bunsen-Ges. Phys. Chem.* **1983**, *87*, 591.

Labowski<sup>3</sup> who had performed measurements between 20 and 4000 MHz discussed the dispersion in the sound velocity of the critical isobutyric acid/water mixture as to be due to relaxation in the concentration fluctuations. Probably, however, these measurements had been performed at too high frequencies to allow for a detection of contributions from chemical reactions with critical anomalies. On the other hand, terms  $(\alpha\lambda)^{\text{ch}}$  with critical slowing down characteristics were also not found in a recent ultrasonic absorption study between 0.2 and 400 MHz of the system 2,6-dimethylpyridine/water with critical composition.<sup>4</sup>

The situation is thus unclear, especially since the theory of Procaccia and Gitterman has been severely criticized recently.<sup>5</sup> It seemed therefore to be of great interest to measure as complete as possible the ultrasonic absorption spectrum of an aqueous isobutyric acid solution of critical concentration and to look for characteristic changes when the temperature is varied toward the critical. Aiming at a reliable identification of the contributions to the total absorption per wavelength (eq 1) with molecular mechanisms we also measured the sound absorption spectra of pure isobutyric acid and of a dilute aqueous solution.

### Experimental Section

**Materials.** Isobutyric acid,  $(\text{CH}_3)_2\text{CHCOOH}$ , was purchased from Fluka (puriss. p.a., >99.5%) and was used without further purification. Water was distilled, additionally deionized, and UV-sterilized. Since the critical point depends sensitively even on slight impurities, the critical composition of the system was determined on the basis of the equal volume criterion of coexisting liquid phases. The value  $y_c = 0.392 \pm 0.001$  (mass fraction of acid) was found. The visually determined phase separation temperature  $T_c = 26.42 \pm 0.02$  °C for the critical mixture was close to the values given in the literature (e.g.,  $T_c = 26.380^\circ\text{C}$ ). The mass fraction of isobutyric acid in the dilute solution was  $y = 0.05$  corresponding to a concentration of about 0.6 mol/L.

**Measurements.** Between 0.2 and 400 MHz the sound absorption coefficient  $\alpha$  of the sample liquids has been determined as a function of frequency  $\nu$  by using three different methods. Below 1 MHz a resonator technique<sup>7</sup> was applied. The  $\alpha$  value was derived from the change in the quality factor resulting if the sample was exchanged for a reference liquid of almost identical sound velocity. At higher frequencies we applied two methods<sup>8</sup> in which pulsed travelling waves were transmitted through a sample of suitable thickness. Between 5 and 30 MHz a fixed path length technique again required appropriately chosen solutions to yield the absorption coefficient relative to a reference. Above 10 MHz another method utilized a cell of variable sample thickness to allow for absolute measurements of  $\alpha$ .

The reactivity of the isobutyric acid solutions made it necessary to exchange some parts of the original specimen cells with some made of inert material even though the acoustic properties of these materials were less favorable. In particular, the transducer crystals of some cells could not be stuck into their fittings with the aid of elastic silicone rubber, but had to be held by a stiffer joint ring made of Teflon. For this reason and also since some of the  $\alpha$  values are unusually high, the experimental accuracy is smaller than with commonly studied liquids. The uncertainty  $\Delta\alpha$  depends on  $\nu$  and  $\alpha$  itself. It may be globally characterized by a value of  $\Delta\alpha/\alpha = 5\%$ . As inferred from the finding that  $\alpha$  values measured with different methods fit to one another, there do not seem to be systematic errors.

### Results and Treatment of Data

**Pure Isobutyric Acid and Dilute Aqueous Solution.** In Figure 1 the ultrasonic absorption spectrum is presented for pure isobutyric acid and also for the dilute aqueous solution. Since the

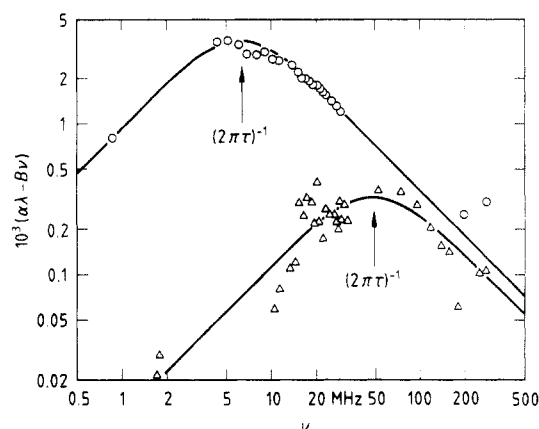


**Figure 1.** Ultrasonic excess absorption per wavelength,  $(\alpha\lambda)^{\text{ex}} = \alpha\lambda - B\nu$ , plotted as a function of frequency  $\nu$  for pure isobutyric acid (O) and for a dilute aqueous solution of isobutyric acid ( $\Delta$ ,  $y = 0.05$ ,  $c \approx 0.6$  mol/L) at 25 °C. The curves represent the corresponding Debye relaxation spectral term (eq 4) with the parameter values according to Table I, respectively.

**TABLE I: Parameters of the Relaxation Spectral Function (Eq 4) for the Dilute Aqueous Solution and for Pure Isobutyric Acid at 25 °C**

$y$	$A, 10^{-3}$	$\tau, \text{ns}$	$B, 10^{-12} \text{ s}$
0.05	$0.63 \pm 0.06$	$3.3 \pm 0.7$	$34 \pm 5$
1	$6.5 \pm 0.1$	$24 \pm 1$	$132 \pm 2$

classical contribution  $(\alpha\lambda)^{\text{cl}}$  is of no interest here, only the excess absorption per wavelength given by

$$(\alpha\lambda)^{\text{ex}} = \alpha\lambda - (\alpha\lambda)^{\text{cl}} \quad (2)$$

is shown in that diagram. In doing so it has been assumed that the classical term according to the relation<sup>9</sup>

$$(\alpha\lambda)^{\text{cl}} = B\nu \quad (3)$$

linearly increases with the frequency  $\nu$ .

The  $(\alpha\lambda)^{\text{ex}}$  vs  $\nu$  relations of pure isobutyric acid and of the dilute aqueous solution both exhibit a relative maximum as characteristic for an underlying relaxation process. As realized by a nonlinear least-squares regression analysis by which the function  $(\omega = 2\pi\nu)$

$$\alpha\lambda(\nu) = \frac{A\omega\tau}{1 + (\omega\tau)^2} + B\nu \quad (4)$$

was fitted to the measured spectra, this relaxation process is characterized by a discrete relaxation time ("Debye process"<sup>10</sup>). The values for the relaxation amplitude  $A$  and for  $\tau$  and  $B$  are given in Table I.

Here and in the following the errors in the parameter values have been established by fitting the model spectral function also to sets of pseudo data  $\tilde{\alpha}\tilde{\lambda}$ . Up to 25 of such sets have been generated per measured spectrum by modification of the original data by using the relation

$$\tilde{\alpha}\tilde{\lambda}(\nu_i) = \alpha\lambda(\nu_i)(1 + r_i\Delta\alpha(\nu_i)/\alpha(\nu_i)) \quad (5)$$

where  $r_i$  ( $-1 \leq r_i \leq 1$ ,  $i = 1, \dots, I$ ) are random numbers,  $I$  is the number of frequencies of measurement, and  $\Delta\alpha(\nu_i)/\alpha(\nu_i) = 0.05$ .

**Mixture of Critical Composition.** The sound absorption spectrum of the isobutyric acid/water mixture of critical composition differs in a characteristic manner from that of the dilute solution and also from that of the pure acid. As demonstrated by Figure 2, where for two different temperatures the  $(\alpha\lambda)^{\text{ex}}$  data of the mixture of critical composition are displayed as a function of  $\nu$ , at least two relaxation mechanisms contribute to the absorption spectrum in the frequency range under consideration. It turns out that the process with the higher relaxation frequency  $((2\pi\tau_2)^{-1}$ , Figure 2), in correspondence to the dilute solution, can

(3) Labowski, M. *Acoust. Lett.* **1979**, *3*, 123.

(4) Kaatze, U.; Schreiber, U. *Chem. Phys. Lett.* **1988**, *148*, 241.

(5) Milner, S. T.; Martin, P. C. *Phys. Rev. A* **1986**, *33*, 1996.

(6) Kolb, H.-A.; Woermann, D. *J. Chem. Phys.* **1984**, *80*, 3781.

(7) Kaatze, U.; Wehrmann, B.; Pottel, R. *J. Phys. E* **1987**, *20*, 1025.

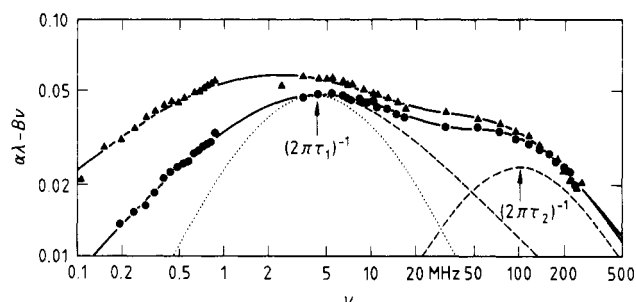
(8) Kaatze, U.; Lautscham, K.; Brai, M. *J. Phys. E* **1988**, *21*, 98.

(9) Edmonds, P. D. *Ultrasonics*; Academic: New York, 1981; p 186.

(10) Debye, P. *Polare Molekeln*; Hirzel: Leipzig, 1929.

**TABLE II: Parameters of the Relaxation Spectral Function (Eq 7) of the Isobutyric Acid/Water Mixture of Critical Composition ( $y = 0.392$ ) at Various Temperatures near the Critical ( $T_c = 26.42$  °C)**

$T, ^\circ\text{C}$	$T - T_c, ^\circ\text{C}$	$A_1$	$\tau_1, \text{ns}$	$\beta$	$A_2$	$\tau_2, \text{ns}$	$B, 10^{-12} \text{ s}$
26.46	0.04	$0.35 \pm 0.02$	$254 \pm 8$	$0.51 \pm 0.05$	$0.041 \pm 0.01$	$3.2 \pm 0.4$	111
26.57	0.15	$0.35 \pm 0.02$	$211 \pm 8$	$0.52 \pm 0.05$	$0.041 \pm 0.01$	$2.0 \pm 0.4$	94
26.68	0.26	$0.36 \pm 0.02$	$237 \pm 8$	$0.54 \pm 0.05$	$0.039 \pm 0.01$	$2.5 \pm 0.4$	109
26.90	0.48	$0.33 \pm 0.01$	$168 \pm 6$	$0.49 \pm 0.03$	$0.039 \pm 0.005$	$2.1 \pm 0.2$	107
27.00	0.58	$0.34 \pm 0.01$	$152 \pm 6$	$0.51 \pm 0.03$	$0.031 \pm 0.005$	$1.9 \pm 0.2$	109
28.00	1.58	$0.30 \pm 0.01$	$129 \pm 6$	$0.49 \pm 0.03$	$0.031 \pm 0.005$	$2.2 \pm 0.2$	106
30.00	3.58	$0.222 \pm 0.004$	$73 \pm 3$	$0.39 \pm 0.03$	$0.036 \pm 0.005$	$1.93 \pm 0.06$	103
35.00	8.58	$0.144 \pm 0.004$	$40 \pm 3$	$0.27 \pm 0.03$	$0.048 \pm 0.005$	$1.58 \pm 0.06$	92

<sup>a</sup>  $\pm 0.02$ . <sup>b</sup>  $\pm 8$ .**Figure 2.** Plot of the ultrasonic excess absorption per wavelength,  $(\alpha\lambda)^{\text{ex}} = \alpha\lambda - B\nu$ , versus frequency  $\nu$  for the isobutyric acid/water mixture of critical composition at 30 °C (▲) and 35 °C (●). Full curves are graphs of the relaxation spectral function defined by eq 7 with the parameter values given in Table II. The dashed curves show for 35 °C the subdivision of the excess absorption spectrum into two contributions, one characterized by a Cole-Cole relaxation time distribution around the principal relaxation time  $\tau_1$ , the other one by the discrete relaxation time  $\tau_2$ . The dotted curve represents a Debye type spectrum with relaxation time  $\tau_1$  and relaxation amplitude  $A_1$ .

be well represented by a Debye term. The  $(\alpha\lambda)^{\text{ex}}$  contributions at lower frequencies, however, extend over a much broader frequency range, thus indicating special features in the underlying mechanism. Moreover, this frequency range dramatically broadens when approaching the critical mixing temperature  $T_c$  (Figure 2).

According to these findings we tried to describe the measured frequency-dependent  $\alpha\lambda$  data by the relation

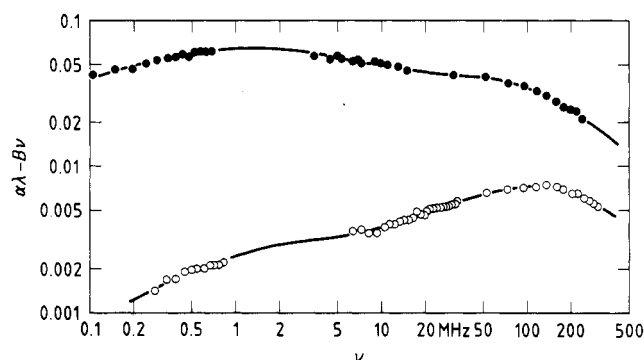
$$\alpha\lambda(\nu) = (\alpha\lambda)^{\text{cf}}(\nu) + \frac{A\omega\tau}{1 + (\omega\tau)^2} + B\nu \quad (6)$$

using for term  $(\alpha\lambda)^{\text{cf}}(\nu)$  the expressions predicted by the theories of either Bhattacharjee and Ferrell<sup>11-13</sup> or of Fixman,<sup>14</sup> Kawasaki,<sup>15</sup> and Mistura et al.<sup>16-18</sup> Other than with the system 2,6-dimethylpyridine/water<sup>4</sup> the theoretical  $(\alpha\lambda)^{\text{cf}}$  vs  $\nu$  functions appeared to be inadequate to describe the present experimental spectra.

Empirically, however, the ultrasonic absorption spectra of the mixture with critical composition at the various temperatures can be well represented by the function

$$\alpha\lambda(\nu) = \frac{1}{2} \frac{A_1 \cos(\beta\pi/2)}{\cosh((1-\beta) \ln(\omega\tau_1)) + \sin(\beta\pi/2)} + \frac{A_2\omega\tau_2}{1 + (\omega\tau_2)^2} + B\nu \quad (7)$$

The first term on the right-hand side of eq 7 reflects an underlying continuous Cole-Cole relaxation time distribution<sup>19</sup>  $G(\tau)$  which,

**Figure 3.** Ultrasonic excess absorption spectrum for aqueous solutions with critical composition of isobutyric acid at 28 °C (●,  $T - T_c = 1.58$  K,  $y_c = 0.392$ ) and of 2,6-dimethylpyridine at 32 °C (○,  $|T - T_c| = 1.40$  K,  $y_c = 0.289$ ).

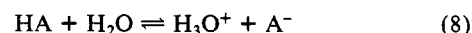
if  $\tau G(\tau)$  is plotted versus  $\ln(\tau/\tau_1)$ , is symmetrically bell-shaped around  $\tau/\tau_1 = 1$ . Parameter  $\tau_1$  denotes the principal relaxation time herein and  $\beta$  measures the width of the relaxation time distribution. Though the Cole-Cole function may be irrelevant from a theoretical point of view, eq 7 is used here for lack of a well-founded expression to analytically describe the measured data. The values for the parameters  $A_1$ ,  $\tau_1$ ,  $\beta$ ,  $A_2$ ,  $\tau_2$ , and  $B$  as found by the nonlinear least-squares fitting procedure are collected in Table II.

It is interesting in this connection that the substitution of the Cole-Cole term in eq 7 by a sum of two Debye terms leads to a less satisfactory representation of the measured spectra though the number of adjustable parameters is increased thereby.

## Discussion

**Cole-Cole Term Strongly Dependent on Temperature.** The inconsistency of the present ultrasonic absorption spectra with the theories describing the critical concentration fluctuations can be illustrated by the comparison of data given in Figure 3. In that diagram  $(\alpha\lambda)^{\text{ex}}$  values at nearly the same  $|T - T_c|$  are displayed as a function of frequency for aqueous mixtures with critical composition of both isobutyric acid and 2,6-dimethylpyridine. In particular at lower frequencies ( $\nu < 20$  MHz) the excess absorption values of the isobutyric acid/water mixture drastically exceed those for the system 2,6-dimethylpyridine/water which are in conformity with the theoretical predictions by Bhattacharjee and Ferrell and also by Fixman, Kawasaki, and Mistura et al.<sup>4</sup> We therefore conclude that in the relevant frequency range below about 20 MHz the spectrum is dominated by contributions resulting from chemical processes and that these contributions mask those due to concentration fluctuations.

The fact that the low-frequency relaxation process is not found in pure isobutyric acid indicates that both solute and solvent molecules participate in the underlying chemical reaction. A possible mechanism may be the dissociation/association process



with HA denoting the acid molecule. Another possible process

- (11) Bhattacharjee, J. K.; Ferrell, R. A. *Phys. Rev. A* **1981**, *24*, 1643.
- (12) Ferrell, R. A.; Bhattacharjee, J. K. *Phys. Lett.* **1981**, *86A*, 109.
- (13) Ferrell, R. A.; Bhattacharjee, J. K. *Phys. Rev. A* **1985**, *31*, 1788.
- (14) Fixman, M. *J. Chem. Phys.* **1962**, *36*, 1961.
- (15) Kawasaki, K. *Phys. Rev. A* **1970**, *1*, 1750.
- (16) D'Arrigo, G.; Mistura, L.; Tortaglia, P. *Phys. Rev. A* **1970**, *1*, 286.
- (17) D'Arrigo, G.; Mistura, L.; Tortaglia, P. *Phys. Rev. A* **1971**, *3*, 1718.
- (18) Mistura, L. In *Critical Phenomena*; Green, M. S., Ed.; Academic: New York, 1971; p 563.

- (19) Cole, K. S.; Cole, R. H. *J. Chem. Phys.* **1941**, *9*, 341.

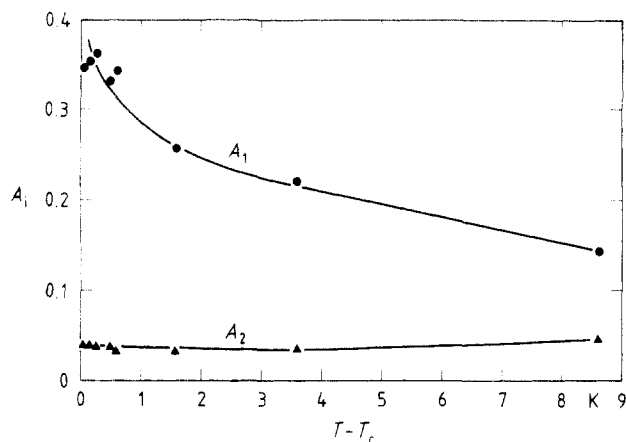


**Figure 4.** Plot of the relaxation amplitudes  $A_1$  (●) and  $A_2$  (▲) of the isobutyric acid/water mixture of critical composition versus the temperature difference  $T - T_c$ .

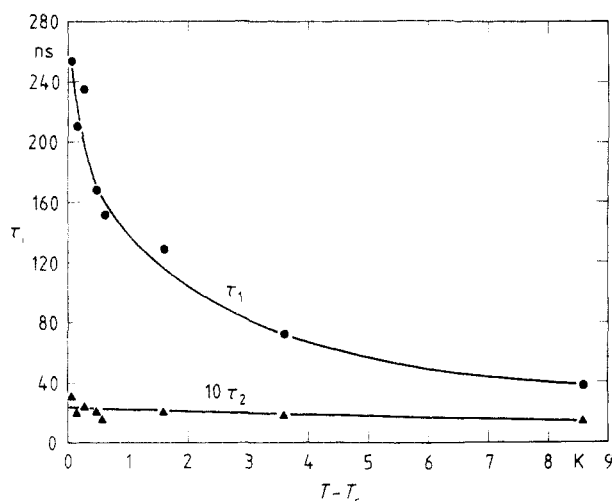


**Figure 5.** Dependence on the temperature difference  $T - T_c$  of the relaxation times  $\tau_1$  and  $\tau_2$  for the aqueous solution of isobutyric acid with critical concentration.

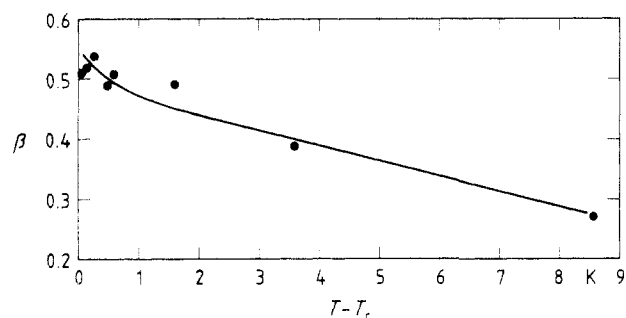


**Figure 6.** Relaxation time distribution parameter  $\beta$  of the low-frequency relaxation process shown as a function of the temperature difference  $T - T_c$  for the isobutyric acid/water mixture of critical composition.

is the formation of molecular aggregates in which rearrangements of the hydrogen bonds between the water and the isobutyric acid molecules are involved.<sup>20-22</sup> The relaxation times associated with both types of elementary reactions are expected to distinctly depend on the concentration and the diffusion coefficient.<sup>23</sup> The existence of a broad relaxation time distribution as indicated by

(20) Lamb, J.; Huddart, D. H. A. *Trans. Faraday Soc.* **1950**, *46*, 540.

(21) Burundukov, K. M.; Podborrov, N. V.; Popov, V. S. *Russ. J. Phys. Chem.* **1973**, *5*, 597.

(22) Kaatze, U.; Woermann, D. *Ber. Bunsen-Ges. Phys. Chem.* **1982**, *86*, 81.

(23) Strehlow, H.; Knoche, W. *Fundamentals of Chemical Relaxation*; Verlag Chemie: Weinheim, 1977.

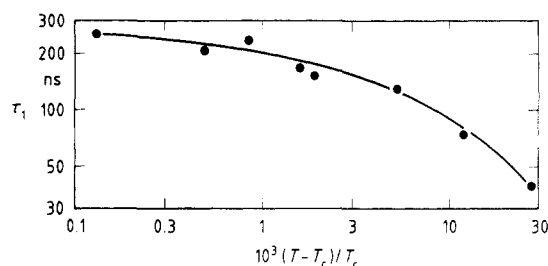


**Figure 7.** Bilogarithmic plot of the relaxation time  $\tau_1$  (Table II) versus the reduced temperature  $(T - T_c)/T_c$ .

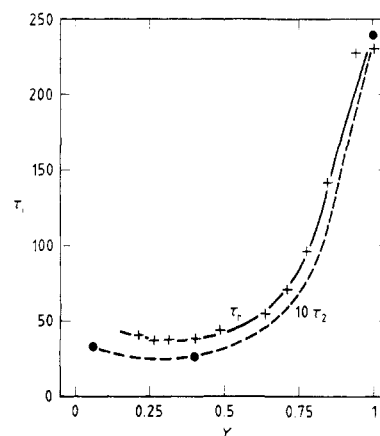
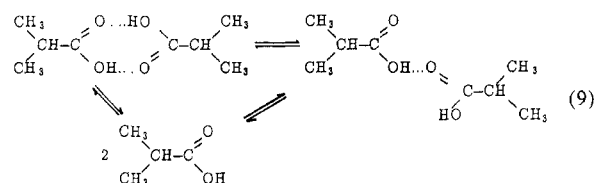


**Figure 8.** Ultrasonic relaxation times  $\tau_1$  (+) and  $\tau_2$  (●) displayed as a function of mass fraction  $\gamma$  of acid for aqueous solutions of acetic<sup>26</sup> and isobutyric acid, respectively. Also included are the values for the pure carboxylic acids. The data refer to 25 °C with the exception of the isobutyric acid mixture of critical composition (27 °C).

the uncommonly high  $\beta$  values is then a consequential reflection of the pronounced spatial and temporal concentration fluctuations near  $T_c$ .

As shown by Figures 4–6 all parameters characterizing the low-frequency relaxation ("1") increase with decreasing  $|T - T_c|$ , that is, with increasing correlation length of local fluctuations in concentration. A bilogarithmic plot of  $\tau_1$  vs the reduced temperature (Figure 7), however, does not define a straight line as predicted by the theory of Procaccia and Gitterman.<sup>1,24,25</sup> This finding may be due to several reasons. On the one hand, measurements have not been performed in the very vicinity of the critical point ( $|T - T_c| \leq 10^{-3}$  K) where theories should especially apply and the frequency range of measurements may be still too small for a sufficient analysis of the broad absorption spectra. On the other hand, as already mentioned above, the Procaccia and Gitterman theory may be incorrect. In the absence of a more detailed theory of sound attenuation in critical mixtures it is thus not possible to decide whether the low-frequency relaxation term found in this study, even though strongly dependent on temperature, does reflect chemical slowing or does not.

**Debye Term Weakly Dependent on Temperature.** The fact that the high-frequency relaxation process ("2" in eq 7) does not only occur in the aqueous solutions but also in the pure isobutyric acid suggests this process to be caused by one of the reaction steps of the dimerization scheme



which is commonly attributed to carboxylic acids. Corsaro and

(24) Hentschel, H. G. E.; Procaccia, I. *J. Chem. Phys.* **1982**, *76*, 666.

(25) Procaccia, I.; Gitterman, M. *Phys. Rev. A* **1983**, *27*, 555.

Atkinson discussed their ultrasonic absorption data between 0.5 and 150 MHz for aqueous solutions of acetic acid in terms of the closed dimer–open dimer reaction.<sup>26</sup> Their relaxation times  $\tau_r$  are displayed as a function of mass fraction  $y$  of acid in Figure 8. A specific  $\tau_r$  vs  $y$  relation is found with a relative minimum at around  $y = 0.3$ , corresponding to an acetic acid concentration of about 6 mol/L. This concentration dependence has been related to stability conditions of the two types of dimers.<sup>26</sup>

As also indicated by Figure 8, our  $\tau_2$  values for the isobutyric acid/water system show a similar dependence on  $y$ . The absolute  $\tau_2$  values, however, are considerably smaller than the relaxation times for the corresponding acetic acid/water mixtures. The present high-frequency ultrasonic relaxation may thus be alternatively assumed to reflect one of the monomer–dimer reactions in the above scheme (eq 9). However, Bader and Plass who measured between 0.3 and 1.5 GHz the sound absorption of pure acetic acid at 20 °C found an additional relaxation process in this frequency range. Its relaxation time has a value of about 0.2 ns.<sup>27</sup>

It seems to be most likely that this fast process is due to the transition between the monomeric and one of the dimeric forms.<sup>27</sup> The high  $B$  values of the isobutyric acid/water system ( $B = 109 \times 10^{-12}$  s at  $y = 0.392$  and 27 °C, Table II;  $B = 31.7 \times 10^{-12}$  s at  $y = 0$  and 25 °C<sup>28</sup>) suggest such a process with a relaxation frequency well above our frequency range of measurements to be also present in these systems. A definite conclusion on the nature of the chemical reaction should be possible on the basis of further ultrasonic absorption studies on different carboxylic acids especially if the measurements can be extended to even higher frequencies.

**Acknowledgment.** We are highly indebted to Professor R. Pottel for his support and encouragement. We also thank Professor D. Woermann, University of Köln, and B. Wehrmann for helpful discussions. Financial support by the Deutsche Forschungsgemeinschaft is gratefully acknowledged.

**Registry No.** Isobutyric acid, 79-31-2.

(26) Corsaro, R. D.; Atkinson, G. *J. Chem. Phys.* 1971, 55, 1971.

(27) Bader, F.; Plass, K. G. *Ber. Bunsen-Ges. Phys. Chem.* 1971, 75, 553.

(28) Lautscham, K. Dissertation, University of Göttingen, 1986.

## Study on Ion–Ion and Ion–Solvent Interactions of Thiocyanates in Water–DMF Mixtures by Raman Spectroscopy

Shinobu Koda,\* Jyuichi Goto, Toshiyuki Chikusa, and Hiroyasu Nomura

Department of Chemical Engineering, School of Engineering, Nagoya University, Chikusa-ku, Nagoya-shi, 464 Japan (Received: August 16, 1988; In Final Form: December 20, 1988)

The Raman spectra of the CS and CN stretching vibrational modes were measured for  $\text{Bu}_4\text{NNCS}$ ,  $\text{NH}_4\text{NCS}$ , and  $\text{LiNCS}$  as a function of DMF content in water–DMF mixtures. In the CS stretching vibrational region, three Raman bands were observed, which were ascribed to the hydrated free  $\text{SCN}^-$  ion, ion-paired  $\text{M–NCS}$  ( $\text{M} = \text{Li}, \text{NH}_4$ ), and the free  $\text{SCN}^-$  ion surrounded by DMF molecules. In the CN stretching vibrational region, Raman bands due to free  $\text{SCN}^-$  ion and ion pair were observed. Discussion on the observations in the CS and CN stretching vibrational modes is made on the basis of the difference in the respective bond character. In addition, information about the vibrational and reorientational motions of  $\text{SCN}^-$  ion in water–DMF mixtures was obtained from the Raman line-shape analysis of the CN stretching vibrational mode. The vibrational motion of  $\text{SCN}^-$  ion strongly depends on the solvent composition but was not so affected by the formation of ion pairs. The reorientational motion is almost independent of the solvent composition and is hindered by ion pair formation.

### Introduction

It is well-known that thiocyanate ion in solutions forms metal–thiocyanate complexes with many cations, such as Co, Ni, Ag, and so on.<sup>1–5</sup> Vibrational frequencies of the CS and CN stretching vibrational modes in  $\text{SCN}^-$  ion are very sensitive to the type of metal complex. The CS vibrational frequency of the  $\text{M–SCN}$  complex shifts to lower frequencies than that of free ion and the vibrational frequency of  $\text{M–NCS}$  complex shifts to higher frequencies. Moreover, the vibrational frequency of the CN stretching mode for the  $\text{M–SCN}$  complex appears at higher values than that for the  $\text{M–NCS}$  complex. The type of the complex is determined by the chemical nature of metal ions.

In nonaqueous solvents, not only simple ion pairs but also dimers and triple ions are formed.<sup>6–18</sup> In order to elucidate the dissolved state of thiocyanates and their complexes, studies of the Raman and infrared spectra of the salts and complexes in solutions have been carried out by many workers.<sup>1–18</sup> Information of dynamic properties of thiocyanate ion in solution is essential to shed light on the ion–ion and ion–solvent interactions and the mechanism of the ion association process. Recently, the dynamic properties of thiocyanate ion have been investigated by ultrasonic and dielectric relaxation methods<sup>19–23</sup> and by Raman line-shape anal-

ysis.<sup>24–26</sup> The thiocyanate ion is a typical linear triatomic ion and belongs to the point group  $C_{\infty v}$ . The Raman line-shape

- (1) Mitchell, P. C. H.; Williams, R. J. P. *J. Chem. Soc.* 1960, 1912.
- (2) Turco, A.; Pecile, C. *Nature* 1961, 66, 191.
- (3) Lewis, J.; Nyholm, R. S.; Smith, P. W. *J. Chem. Soc.* 1961, 4590.
- (4) Irish, D. E. In *Ionic Interactions*; Petrucci, S., Ed.; Academic Press: New York, 1971; Vol. 3, p 187.
- (5) Nakamoto, K. *Infrared and Raman Spectra of Inorganic and Coordination Compounds*, 3rd ed.; Wiley: New York, 1978; p 270.
- (6) Pecile, C. *Inorg. Chem.* 1965, 5, 210.
- (7) Chabanel, M.; Ménard, C.; Guihéneuf, G. C. R. *Acad. Sci. Paris, Ser. C* 1971, 272, 253.
- (8) Ménard, C.; Wojtkowiak, B.; Chabanel, M. *Bull. Soc. Chim. Belg.* 1972, 81, 241.
- (9) Paoli, D.; Chabanel, M. C. R. *Acad. Sci. Paris, Ser. C* 1977, 284, 95.
- (10) Paoli, D.; Lucon, M.; Chabanel, M. *Spectrochim. Acta* 1978, 34A, 1087.
- (11) Paoli, D.; Lucon, M.; Chabanel, M. *Spectrochim. Acta* 1979, 35A, 593.
- (12) Chabanel, M.; Lucon, M.; Paoli, D. *J. Phys. Chem.* 1981, 85, 1058.
- (13) Chabanel, M.; Wang, Z. *J. Phys. Chem.* 1984, 88, 1441.
- (14) Chabanel, M.; Wang, Z. *Can. J. Chem.* 1984, 62, 2320.
- (15) Rannou, J.; Chabanel, M. *Inorg. Chem.* 1985, 24, 2319.
- (16) Bacelon, P.; Corset, J.; de Loze, C. *J. Solution Chem.* 1980, 9, 129.
- (17) Bacelon, P.; Corset, J.; de Loze, C. *J. Solution Chem.* 1983, 12, 1, 13, 23.
- (18) Lemley, A. T.; Lagowski, J. J. *J. Phys. Chem.* 1974, 78, 708.
- (19) Irish, D. E.; Tang, S.-Y.; Talts, H.; Petrucci, S. *J. Phys. Chem.* 1979, 83, 3268.

\* To whom correspondence should be addressed.